Fabrication and Paracrine Effect Research of Bone Marrow-Derived Endothelial Progenitor Cell Sheet

Fenlong Xue
Tianjin First Central Hospital
Yuanfeng Xin
Shanghai Oriental Hospital and Tongji University Affiliated Oriental Hospital
Yunpeng Bai
Tianjin Chest Hospital
Yiyao Jiang
The First Affiliated Hospital of Bengbu Medical College
Jianhsi Liu
Deltahealth hospital of shanghai
Kaitao Jian (kaitao.jian@outlook.com)
Deltahealth hospital of shanghai https://orcid.org/0000-0002-4856-3342

Research

Keywords: Endothelial Progenitor Cell (EPC), Cell sheet, SDF-1α/CXCR4 axis, Paracrine

Posted Date: October 29th, 2020

DOI: https://doi.org/10.21203/rs.3.rs-97639/v1

Abstract

Background: The release of a wide array of endothelial progenitor cell (EPC) sheet-secreted paracrine factors is central to the mechanism by which these cells contribute to tissue repair. The purpose of this study was to fabricate BM-EPC sheet and conduct preliminary investigation on the paracrine effect of SDF-1 about the role of the stromal cell-derived factor-1α (SDF-1α)/CXCR4 axis in the form of tubular structures from BM-EPCs sheet.

Methods: EPCs derived from rat bone marrow (BM-EPC) were identified and isolated by the cell-surface markers CD34/CD133/VE-cadherin/KDR using flow cytometry, as well as by dual affinity for acLDL and UEA-1. Single-cell suspensions were seeded on temperature-responsive cell culture dishes. After 7 days of incubation, the BM-EPC cells were easily harvested as cell sheets, and a series of biochemical experiments were performed in vitro. The expression levels of SDF-1α/CXCR4 axis-associated genes and proteins were examined using RT-qPCR and western blot analysis, and enzyme-linked immunosorbent assay (ELISA) was applied to determine the concentrations of VEGF, EGF and SDF-1α in the cell culture medium.

Results: The BM-EPC cell sheets were successfully harvested. Moreover, BM-EPC cell sheets have superior proliferation and tube formation activity when compare with single cell suspension. When capillary-like tube were formed from EPCs sheets, the releasing of paracrine factors such as VEGF, EGF, and SDF-1 were increasing. To drive the tube formation of BM-EPCs sheets, our mechanism research showed that the activation of PI3K/AKT/eNOS pathway since the phosphorylation of protein CXCR, PI3K, AKT and eNOS were increasing.

Conclusion: BM-EPC cell sheets have superior proliferation and tube formation activity that can be used for tissue repair. The strong ability to secrete paracrine factors was be related to the SDF-1α/CXCR4 axis through PI3K/AKT/eNOS pathway.

Introduction

The Endothelial Progenitor Cells (EPC) treatment strategy take advantages of preserving or regenerating tissue to develop towards clinical application[1–3]. However, the disadvantage of single cells transplantation related aggregation and necrosis make the the feasibility and effectiveness of the approach remain insufficient and difficult in clinical trials[4, 5]. EPC derived from bone marrow (BM-EPC) sheet are known to play an important role in angiogenesis by participating not only in the formation of vessels but also in vessel repair and remodeling[6, 7]. It can release a wide array of paracrine factors to fabricate tissue repair. However, the forming of BM-EPC sheet and the action characteristics of forming tubular structures remain unclear.

Several studies have demonstrated that SDF-1 expression is sufficient to induce EPC cell mobilization and enhance angiogenesis[8]. CXCR4, which is the main SDF-1 receptor, is widely expressed on BM-EPCs. The SDF-1α/CXCR4 axis has been well documented to play a significant role in BM-EPC mobilization and

has also been reported to be correlated with the proliferation and survival of EPCs[9, 10]. Accumulating evidence has indicated that the phosphatidylinositol 3-kinase (PI3K)/AKT signaling pathway is stimulated to participate in EPC cell proliferation and tube formation capacity. SDF-1α/CXCR4 could also decrease EPC cell apoptosis under serum deprivation or hypoxic conditions via the PI3K/AKT/eNOS pathway[10, 11]. Some animal studies indicated that BM-EPC cell sheet technology increased vasculogenesis[12]. However, BM-EPCs cell sheet can not harvested with trypsin and cell-to-cell interactions and the integral structure of the BM-EPCs sheet were unknown[13, 14].

Our groups focused on tissue repair for several years and we found tube formation of BM-EPCs sheets was associated with increasing secretion of SDF-1α, EGF and VEGF. VEGF and EGF can acted as paracrine factors to promote BM-EPCs sheets tube forming[15, 16], while the effect of SDF-1 was still unknown. Based on the pro-angiogenic effect of SDF-1[17] and effect characteristics of tube forming from BM-EPCs sheets, we hypothesize BM-EPCs can form tubular structures via the paracrine activity of SDF-1α/CXCR4 axis.

Materials And Methods

Animals

This study was reviewed and approved by the Animal Ethics Committee of Tianjin First Central Hospital. Adult Wistar rats, 8 weeks of age (weighing 250-280 g), were purchased from the experimental animal center of the Military Academy of Medical Sciences, China. All surgical procedures and care administered to the animals were approved by the Animal Care Committee and performed according to institutional guidelines.

Isolation and culturing of BM-EPCs

Wistar rats were sacrificed by decapitation and soaked in 75% ethanol twice.

Mononuclear cells were isolated from rat BM, especially femur and tibia of the rats, by density gradient centrifugation using Histopaque 1083(Sigma, Stlouis, USA). Isolated cells were resuspended in M199 medium(Gibco, Carlsbad, USA, involved 10% FBS, 20% double antibody, 20 ng/ml VEGF (Sigma), and 1 ng/ml bFGF (Sigma)) and cultured in fibronectin-coated dishes and maintained at a 37℃+5% CO_2 incubator. After 4 days in culture, non-adherent cells were removed and fresh medium was added. After the 7 days of culture, BM-EPC cells were identified by a combination of specific surface marker expression.

a. Identification of BM-EPCs by endothelial marker

Afer 7 days of incubation, the adherent cells were digested by 0.25% trypsin and counted 2×10^6 cells. Aliquotes containing 1×10^6 cells/100μL into each tubes, were added primary antibody at an appropriate dilution and incubate for 2 h at room temperature. These endothelial markers include CD133 (Proteintech

Group, Inc, WuHan, China), CD34 (Proteintech Group, Inc, WuHan, China), VE-cadherin (Bioss, Beijing, China), and KDR (Proteintech Group, Inc, WuHan, China). Then add diluted secondary antibody to the cells and incubate for 1 h at room temperature. The surface markers on BM- EPCs was analyzed by the flow cytometry (BD bioscience, USA), data was analyzed using BD CellQuest™ Pro software Version 5.1.

Identification of BM-EPCs by immunochemistry

The fibronectin-adherent BM- Derived EPCs were identified by incubation with 10μg/ml of fluorescently labeled acetylated-low density lipoprotein (Dil-ac-LDL; Molecular Probes, Eugene, OR, USA) for 4h and 10μg/ml of fluorescently FITC labeled Ulex Europaeus Agglutinin 1 (UEA-1; Sigma-Aldrich, MS, USA) for 1h at room temperature, then co-incubation with DAPI for 15 min, Images were captured by inverted fluorescence microscopy (Olympus IX71, Olympus Optical Co. Ltd, Tokyo, Japan), Double positive cells can be considered BM-EPCs.

The BM-EPCs transwell to SDF-1α assey

Resuspend the cells to 5×10^4/100μL and coated into 24-well Millipore Transwell chambers. 100μL suspension were coated in upper chambers, meanwhile 600μL SDF-1α (R&D Systems, Inc, USA)solution was injected into the lower chambers with the concentration of 1ng/ml, 10 ng/ml and 100 ng/ml, respectively. Incubated the Millipore Transwell chambers at 37℃ for 45-60 min. Discarded the solution of chambers, washed with 1×PBS and fixed in 4% paraformaldehyde with 600μL for 30 min. Stained with 600μL 0.1% crystal violet for 20 min. Finally, Images were captured by fluorescence microscopy (Leica Microsystems, Wetzlar, Germany).

Fabrication of BM-EPC cell sheets and thickness assey

1.5×10^6 BM-EPCs were seeded into Nunc UpCell Surface dishes (Thermo Scientific, USA) coated with vitronectin. Under temperature-responsive culture, incubated for 37℃and 7 days firstly, then reducing the temperature to 25℃ for 30 min, the cells spontaneously detached as contiguous cell sheets and were harvested from the dishes.

To observe detached EPCs sheets thickness, one sheet were fixed with 20 mL -20℃ ice-cold methanol solution under 4℃for10 min,3ml primary Anti-Collagen I antibody (1:300,Bioss,Beijing Biosynthesis Biotechnology, Beijing, China) were added to the dishes. After incubation for 5 min at 37℃, 3ml secondary antibody Alexa Flour 488 (1:500, Proteintech Group, Inc, WuHan, China) were injected, incubate at 37℃in the dark for 1 h. Cell nuclei were visualized with DAPI after incubation with secondary antibodies. Images were obtained using fluorescence microscope.

BM-EPC cell sheets proliferation assay.

The proliferative capacity of the BM-EPCs sheets was measured using a Cell Counting Kit-8 (CCK-8, Dojindo Laboratories, Japan) assay. 5×10^3/well were seeded into 96-well plates and maintained at a 37℃atmosphere. At the indicated time points (cultivated after 12h,24h,48h and 72h),10 μl Cell Counting

Kit-8 was added to each well and cells were cultured for an additional 4 h. Finaly, an enzyme immunoassay analyzer was used to measuring the optical density (OD) at an absorbance wavelength of 450 nm. In order to compare the proliferative capacity of the BM-EPCs sheets, EPCs were used as control.

BM-EPC cell sheets tube formation assay

The BM-EPCs and BM-EPC cell sheets (2 x 10^4 cells) maintained in M199 medium(Sigma-Aldrich, USA) were seeded onto Matrigel(Corning Matrigel Basement Membrane Matrix,Corning,USA)-coated 96-well plates and further cultured in 37°Cfor 4 h, respectively. To compare the capillary-like tube formation of EPCs sheets and BM-EPCs, Microscope images were captured using inverted phase-contrast microscopy (IX71; Olympus), and the number of network circles for each groups in each image was counted using the Wimasis image analysis program.

Reverse transcription-quantitative PCR (RT-qPCR)

Respectively, total RNA from BM-EPCs and BM-EPCs sheets (1.5×10^6 cells) was extracted using RNAiso Plus (TaKaRa Biotechnology, Japan) according to the manufacturer's protocol. Total RNA was converted into cDNA using PrimeScript^{TM} RT Reagent Kit (TaKaRa Biotechnology, Japan), under the following condition: 37°C for 15 min, 85°C for 5 sec and 4°C for 5 min. cDNA was amplified under SYBR Premix Ex Taq^{TM} (TaKaRa Biotechnology, Japan).The sequences of the primers are shown as follows (Table 1) The qPCR thermocycler conditions were as follow：firstly：95°C for 30 s, followed by 40 cycles of 95°C for 5 s and 60°C for 30 s. β-actin were used as internal reference and relative mRNA expression levels were calculated using the $2^{-\Delta Ct}$ (fold difference), whereΔCt = (Ct of target genes)-(Ct of endogenous control gene, β-action) in experimental samples.

Western blot analysis of CXCR4/p-CXCR4、PI3K/p-PI3K、AKT/p-AKT、eNOS in BM-EPCs and BM-EPC cell sheets

Respectively, total protein was extracted from BM-EPCs and BM-EPCs sheets(1×10^6 cells) and quantified using the BCA Protein Assay Kit (TaKaRa, Japan).Proteins lysates were isolated by using 10% SDS-PAGE and then transferred them to PVDF membrane (Millipore, USA).The membrane were incubated with the antibodies against CXCR4 (1:1000; Proteintech Group, Inc, WuHan, China)、 P-CXCR4 (1:1000; Bioss, Beijing, China.)、PI3K(1:1000;Abcam,USA.ab86714)、P-PI3K(1:1000; Abcam,USA.ab182651)、AKT(1:500; Proteintech Group, Inc, WuHan, China)、P-AKT(1:3000; Proteintech Group, Inc, WuHan, China)、eNOS (1:300; Bioss, Beijing, China) and Tubulin(1:200; Proteintech Group, Inc, WuHan, China). HRP-conjugated Affinipure Goat Anti-Rabbit IgG(H+L) was used as secondary antibodies. The signals were quantified with Image Studio.

Detection the expression of paracrine factors SDF-1α, VEGF and EGF using ELISA

The BM-EPCs and BM-EPC cell sheets (1x10^6 cells) were incubated in M199 medium which were serum- and growth factor-free under 37°C+5% CO_2 atmosphere for 7 d. According to the manufacturer's protocol,

the medium was subsequently collected to discover the expression of paracrine factors SDF-1α, VEGF and EGF using ELISA kit. ELISA Kit information is as follows: Rat SDF-1α ELISA kit (Quanzhou Konodi Biotechnology Co. Ltd, China), Rat VEGF ELISA kit (Quanzhou Konodi Biotechnology Co. Ltd, China), Rat EGF ELISA kit (Quanzhou Konodi Biotechnology Co. Ltd, China). The absorbance at 450 nm was measured.

Statistical analysis.

Statistical analyses were conducted using SPSS software version 20.0. Data are expressed as the mean ± standard deviation (SD). Comparisons between two groups were analyzed by a paired samples *t*-test. Comparisons between groups were analyzed with one-way analysis of variance (ANOVA), following by the least significant difference test (LSD-*t*). *p* values of less than 0.05 were considered significantly different.

Results

Characterization of BM-EPCs

The BM-EPCs were cultured for 7 days and had a cobblestone-like appearance (Figure 1 A, B). After expansion in an incubator for 7 days, BM-EPCs showed the ability to incorporate DiI-acLDL (Figure 1D) and bind UEA-1(Figure 1C), and these dual-stained cells can be considered to exhibit the proliferative characteristics of BM-EPCs, as presented in Fig 1F. BM-EPCs were identified by CD34, CD133, KDR, and VE-cadherin using flow cytometry, as presented in Figure 1G. This information indicated that the cultured cells were BM-EPCs.

Functional analysis of BM-EPC migration toward SDF-1α in a Transwell assay

To further confirm the function of BM-EPCs, the directed migration potential of EPCs was detected by a Transwell assay with migration toward SDF-1α. As shown in Figure 2, rat BM-EPCs exhibited directional migration to SDF-1α. Under non-SDF-1α conditions, BM-EPCs were able to migrate through the filter at a low rate of 133.33±4.99 cells per field of view. As the concentration of SDF-1α in the lower chambers increased, the chemotaxis of EPCs became more obvious (Figure 2 E). There were significant differences in the level of SDF-1α between the 10 ng/ml group (180.67±7.72 cells per field of view) and the other groups ($p=0.0$ *vs* 0 ng/ml group; $p=0.009$ *vs* 1 ng/ml group; $p<0.05$). Compared with 10 ng/mL SDF-1α codition, BM-EPCs, under the 100 ng/ml SDF-1α condition, showed the highest rate of migration through the filter (185.33±9.29 cells per field of view), but this difference did not reach statistical significance($p=0.499$).

Gross examination of BM-EPC sheets

After inoculation on temperature-responsive culture plates, the cells spontaneously detached as contiguous cell sheets and were harvested. The gross examination of BM-EPC cell sheets is shown in Figure 3. As shown in the pictures, the EPCs were remarkably connected (Figure 3A). The EPC sheets were

irregular in shape and polygonal (Figure 3B, C). Under a fluorescence microscope, the thickness of the single-layer cell sheet was approximately 15 μm (Figure 3D). The multilayer cell sheet with approximately 3-4 layers was 60 μm (Figure 3E).

The cell sheet system accelerates cell proliferation and cell tube formation in vitro

A Cell Counting Kit-8 (CCK-8) assay was used to quantify the levels of cell proliferation. The OD values of the EPC sheet groups were increased compared with those of the EPC groups. In addition, with increasing time within 24 h, the cells in the EPC cell sheet group grew at a significantly faster rate than did the cells in the EPCs groups (Figure 4C). After 24 h, the cells in the EPC sheet proliferated slowly and initiated apoptosis, but the proliferation rate was not obvious in the EPC groups. Using the in vitro model of angiogenesis, we assessed the capacity of the two groups to form tubular structures. After seeding onto Matrigel for incubation for 4 h, the EPC groups exhibited almost no tube formation (Figure 4B), whereas the EPC sheet groups formed significantly more complete tubes (Figure 4A). Quantitative analysis showed that the total number of tubes formed by the EPC sheet groups (29.33±5.13) was significantly greater than that formed by the EPC group (6.67±4.61 and $p<0.05$).

The expression of CXCR4, PI3K, AKT, and eNOS in EPC sheets

We examined the mRNA expression of genes in the SDF-1α/CXCR4 axis in BM-EPC cell sheets and EPCs by RT-qPCR. RT-qPCR analysis showed that there was no significant difference in CXCR4, PI3K, or AKT mRNA levels between the BM-EPC cell sheets and EPCs groups (Figure 5A, B, C). Interestingly, the level of eNOS expression was significantly higher in the BM-EPC cell sheets groups than in the EPCs groups (Figure 5 D, $p=0.001$). To explore whether the SDF-1α/CXCR4 signaling pathway plays a positive role in paracrine BM-EPC cell sheets, western blotting was used to analyze the difference in protein expression in the two groups (Figure 5E-H). The results showed that the phosphorylation of protein CXCR, PI3K, AKT, eNOS was increasing in the BM-EPC cell sheets groups that form tubular structures when compared with the EPCs groups. These protein was located in PI3K/AKT/eNOS pathway, and downstream of the SDF-1α/CXCR4 axis. These results indicated BM-EPC cell sheets form tube was associated with the activation of SDF-1α/CXCR4 axis and PI3K/AKT/eNOS pathway.

BM-EPC cell sheets promoted the paracrine factors VEGF, EGF, and SDF-1α

Furthermore, to detect the differences in paracrine factors between the two groups, we applied ELISA to determine the concentrations of VEGF, EGF and SDF-1α in the cell culture medium (Figure 6 A-C). The results showed that the expression levels of VEGF (194.72±8.00 pg/ml vs 163.07±2.68 pg/ml), EGF (298.33±1.17 pg/ml vs 288.17±1.51 pg/ml) and SDF-1α (5.21±0.02 pg/ml vs 4.84±0.03 pg/ml) protein in the BM-EPC cell sheets groups were significantly higher than those in the EPCs groups ($p=0.002$, $p=0.001$ and $p=0.00$, respectively). Based on the paracrine of VEGF and EGF, as well as the activation of SDF-1α/CXCR4 axis, we speculated the form of tubular structures from BM-EPCs sheet was associated with the increasing paracrine effect of VEGF, EGF and SDF-1α.

Discussion

Although the exact definition of BM-EPC cells remains unclear in terms of specific surface markers, the vasculogenic, angiogenic, and beneficial paracrine effects of transplanted BM-EPC cells in the treatment of ischemic diseases cannot be overlooked[18].The most widely accepted typical definition is the coexpression of the cell-surface markers CD34/CD133/VE-cadherin/KDR[19].In the present study, stem cell markers and endothelial cell markers, $CD34^+/CD133^+/VE\text{-}cadherin^+$ /KDR^+, were used to identify and isolate the BM- EPC cells by flow cytometry, as well as dual affinity for acLDL and UEA-1[20]. The results revealed that the isolated and cultured cells exhibited typical characteristics of BM-EPCs. Moreover, BM-EPCs sheets formed tubular structures in the in vitro model of angiogenesis.

SDF-1α, which mediates many disparate processes exclusively via a single cell surface receptor known as chemokine receptor CXCR4, has been found to promote BM-EPC cell mobilization into the ischemic site, where they promote repair by inducing vasculogenesis and secreting beneficial paracrine factors [8, 21, 22]. Following verification of the migration potential of EPCs, the data from the present study indicated that a dose of 10 ng/ml SDF-1α is the optimal concentration for BM-EPC cell proliferation. The SDF-1α/CXCR4 axis is important for the homing or recruitment of circulating EPCs in response to hypoxia or injury[23]. Recent studies have supported the central role of the SDF-1α/CXCR4 axis in regulating the mobilization of BM-EPC cells and its potential significance in cardiac repair through induction of angiogenesis and cardioprotective functions after myocardial infarction[24], as well as several intracellular signaling pathways[25]. Among these signals, the *PI3K/AKT* pathway plays a very important role by stimulating growth factor production and adhesion molecule interactions, including the activation of endothelial nitric oxide synthesis (eNOS) activity, which has been confirmed to decrease EPC cell apoptosis[11, 26].

Cell sheets, whose composition is similar to that of natural tissues, are harvested without enzyme treatment, and cell-to-cell interactions and the sheet structure are well preserved. Compared with traditional cell suspension injection methods, in which most of the cells are washed-out into blood vessels and can may die due to the locally harsh ischemic microenvironment, cell sheet technology has been widely used in regenerative medicine as a novel method of cell therapy[14, 27, 28]. BM-EPCs cells, which have the advantage of a higher proliferation rate and can facilitate vessel formation and produce pro-angiogenic factors to enhance vascularization after implantation, have been regarded as an ideal candidates to address vascular issues alonely or in cocultured with other cells. Recently, Kawamura et al. reported that MSCs and BM-EPC cells, as colayered cell sheets, prevented cardiac dysfunction and microvascular disease[12]. Another study showed that EPC-SMC bilevel cell sheet technology facilitated the natural interaction between EPCs and SMCs, thereby creating a structurally mature, functional microvasculature in a rodent ischemic cardiomyopathy model, leading to improved myocardial function[29].

Previous research has shown that the release of a wide array of EPC-secreted paracrine factors is central to the role of EPCs in myocardial repair[30, 31], however, signaling pathways related to paracrine factors

are rarely reported[32]. This limited but valuable information hints at the potential relation between paracrine factor secretion and the SDF-1α/CXCR4 axis. We hypothesized that the SDF-1α/CXCR4 axis might have been activated by a paracrine mechanism, through the *PI3K/AKT* pathway. In this study, we seeded BM-EPCs in suspension on temperature-responsive cell culture dishes and cultured them for 7 days. After 7 days of incubation, the cultured BM-EPC cells had a polygonal cobblestone shape and were easily harvested as a cell sheet, and a series of biochemical experiments were performed in vitro. We found that the levels of cell proliferation and tube formation in the BM-EPC cell sheet group were remarkably increased compared with those in the single-cell groups. To further explore the signaling pathway involved in the mechanism of paracrine action in vitro, the expression levels of SDF-1α/CXCR4 axis-associated genes and proteins were examined using RTqPCR and western blot analysis, respectively. We found that the levels of genes associated with the *PI3K AKT* pathway were not different between the two groups; however, in accordance with previous studies on protein levels of factors associated with this pathway, our present study indicated that the levels of PI3K/AKT/eNOS were all augmented in the BM-EPC cell sheet groups. The data from the present study implied that the SDF-1α/CXCR4 axis may accelerate cell proliferation and decrease apoptosis in the cell sheet system[33,34].

Previous studies suggested that the functional benefits observed after EPC cell transplantation in experimental animal models of myocardial infarction might be related to the secretion of paracrine factors. These factors include factors that promote neovascularization, anti-inflammation effects, promoting cell migration and proliferation, as well as other known or unknown factors[35, 36], such as SDF-1, insulin-like growth factor-1, hepatocyte growth factor (HGF), epidermal growth factor (EGF),VEGF, and IL-8 among many others. VEGF, which is a strong promoter of angiogenesis and neovascularization, is important for EPC cell differentiation, migration, proliferation and vascular remodeling, as can be concluded from previous studies[7, 37]. SDF-1α, together with its receptor CXCR4, is crucial for BM-EPC mobilization from the bone marrow to the peripheral blood circulation and is important in cardiogenesis and vasculogenesis[7, 36, 38]. EGF plays a vital role in cell proliferation and differentiation by binding with EGF receptors. In the past few decades, it has been reported that EPCs provide protection by paracrine mechanisms involving release of a wide array of cytokines. In the present study, we have found that many important cytokines for regulating cell proliferation, survival, and the angiogenic process were clearly detected in the supernatants of BM-EPC cell sheets after 7 days of cultivation.

There are, however, still some problems to overcome for clinical application and some limitations of this study. One of the limitations is that the results presented in this study were obtained from in vitro experiments but not animal models. Another limitation is that the results of our study showed that the SDF-1α/CXCR4 axis may promote the secretion of paracrine factors; however, multiple mechanisms may involved in the paracrine action and the crosstalk of these paracrine factors was still unknown. Indeed, more detailed and specific signaling research should be performed in future trials.

Conclusions

We successfully obtained BM-EPC cell sheets and confirmed that the sheets have superior proliferation and tube formation activity compared to those of EPC single-cell suspensions *in vitro*. The detailed research results showed that the SDF-1α/CXCR4 axis may promote the secretion of the paracrine factors VEGF, EGF and SDF-1α.

Declarations

Ethics approval and cinsent to participate:

This study was reviewed and approved by the Animal Ethics Committee of Tianjin First Central Hospital (Number:E2017087L).

Consent for publication:

Not applicable

Availability of data and materials:

The datasets used and/or analyzed during the current study are available from the corresponding author on reasonable request.

Competing Interests

The Authors declare that they have no conflict of interests

Funding:

This work was supported by grants from the Natural Science Foundation of Tianjin (Grants Number: 16JCYBJC23300), National Natural Science Foundation of China (Grants Number: 81800214)

Acknowledgments:

Not applicable

Authors' contributions:

Fenlong Xue-Writing, Data collection,Statistics and Draft

Yuanfeng Xin-Data collection,Statistics

Yunpeng Bai-Finish the experiment,Data collection

Yiyao Jiang-Data collection

Jianshi Liu-Reviewing

Kaitao Jian-Reviewing, Data collection,Statistics and Draft

References

1. Li M, Ma J, Gao Y, Yang L. Cell sheet technology: a promising strategy in regenerative medicine. Cytotherapy 2019; 21: 3-16.
2. Guo R, Morimatsu M, Feng T, Lan F, Chang D, Wan F, et al. Stem cell-derived cell sheet transplantation for heart tissue repair in myocardial infarction. Stem Cell Res Ther 2020; 11: 19.
3. Kim SR, Yi HJ, Lee YN, Park JY, Hoffman RM, Okano T,et al. Engineered mesenchymal stem-cell-sheets patches prevents postoperative pancreatic leakage in a rat model. Sci Rep 2018; 8: 360.
4. Menasché P. Cell therapy trials for heart regeneration - lessons learned and future directions. Nat Rev Cardiol 2018; 15: 659-671.
5. Haraguchi Y, Shimizu T, Sasagawa T, Sekine H, Sakaguchi K, Kikuchi T,et al. Fabrication of functional three-dimensional tissues by stacking cell sheets in vitro. Nat Protoc 2012; 7: 850-858.
6. Liman TG, Endres M. New vessels after stroke: postischemic neovascularization and regeneration. Cerebrovasc Dis 2012; 33: 492-499.
7. Esquiva G, Grayston A, Rosell A. Revascularization and endothelial progenitor cells in stroke. Am J Physiol Cell Physiol 2018; 315: C664-C674.
8. Cheng M, Huang K, Zhou J, Yan D, Tang YL, Zhao TC,et al. A critical role of Src family kinase in SDF-1/CXCR4-mediated bone-marrow progenitor cell recruitment to the ischemic heart. J Mol Cell Cardiol 2015; 81: 49-53.
9. Shen L, Gao Y, Qian J, Sun A, Ge J. A novel mechanism for endothelial progenitor cells homing: The SDF-1/CXCR4-Rac pathway may regulate endothelial progenitor cells homing through cellular polarization. Med Hypotheses 2011; 76: 256-258.
10. Zheng H, Dai T, Zhou B, Zhu J, Huang H, Wang M, et al. SDF-1alpha/CXCR4 decreases endothelial progenitor cells apoptosis under serum deprivation by PI3K/Akt/eNOS pathway. Atherosclerosis 2008; 201: 36-42.
11. Zhang Y, You B, Liu X, Chen J, Peng Y, Yuan Z. High-Mobility Group Box 1 (HMGB1) Induces Migration of Endothelial Progenitor Cell via Receptor for Advanced Glycation End-Products (RAGE)-Dependent PI3K/Akt/eNOS Signaling Pathway. Med Sci Monit 2019; 25: 6462-6473.
12. Kawamura M, Paulsen MJ, Goldstone AB, Shudo Y, Wang H, Steele AN, et al. Tissue-engineered smooth muscle cell and endothelial progenitor cell bi-level cell sheets prevent progression of cardiac dysfunction, microvascular dysfunction, and interstitial fibrosis in a rodent model of type 1 diabetes-induced cardiomyopathy. Cardiovasc Diabetol 2017; 16: 142.
13. Zhou S, Yang R, Zou Q, Zhang K, Yin T, Zhao W, et al. Fabrication of Tissue-Engineered Bionic Urethra Using Cell Sheet Technology and Labeling By Ultrasmall Superparamagnetic Iron Oxide for Full-Thickness Urethral Reconstruction. Theranostics 2017; 7: 2509-2523.

14. Lu Y, Zhang W, Wang J, Yang G, Yin S, Tang T, et al. Recent advances in cell sheet technology for bone and cartilage regeneration: from preparation to application. Int J Oral Sci 2019; 11: 17.
15. Hassanzadeh H, Matin MM, Naderi-Meshkin H, Bidkhori HR, Mirahmadi M, Raeesolmohaddeseen M, et al. Using paracrine effects of Ad-MSCs on keratinocyte cultivation and fabrication of epidermal sheets for improving clinical applications. Cell Tissue Bank 2018;19: 531-547.
16. Ryu B, Sekine H, Homma J, Kobayashi T, Kobayashi E, Kawamata T, et al. Allogeneic adipose-derived mesenchymal stem cell sheet that produces neurological improvement with angiogenesis and neurogenesis in a rat stroke model. J Neurosurg 2019; 132: 442-455.
17. Spinetti G, Sangalli E, Specchia C, Villa F, Spinelli C, Pipolo R et al. The expression of the BPIFB4 and CXCR4 associates with sustained health in long-living individuals from Cilento-Italy. *Aging (Albany NY)*. 2017;9(2):370-380.
18. Peters EB. Endothelial Progenitor Cells for the Vascularization of Engineered Tissues. Tissue Eng Part B Rev 2018; 24: 1-24.
19. Hirschi KK, Ingram DA, Yoder MC. Assessing identity, phenotype, and fate of endothelial progenitor cells. Arterioscler Thromb Vasc Biol 2008; 28: 1584-1595.
20. Asahara T, Murohara T, Sullivan A, Silver M, van der Zee R, Li T, et al. Isolation of putative progenitor endothelial cells for angiogenesis. Science 1997; 275: 964-967.
21. Patry C, Stamm D, Betzen C, Tönshoff B, Yard BA, Beck GC, et al. CXCR-4 expression by circulating endothelial progenitor cells and SDF-1 serum levels are elevated in septic patients. J Inflamm (Lond) 2018; 15: 10.
22. Petit I, Jin D, Rafii S. The SDF-1-CXCR4 signaling pathway: a molecular hub modulating neo-angiogenesis. Trends Immunol 2007; 28: 299-307.
23. Kawakami Y, Ii M, Matsumoto T, Kuroda R, Kuroda T, Kwon SM, et al. SDF-1/CXCR4 axis in Tie2-lineage cells including endothelial progenitor cells contributes to bone fracture healing. J Bone Miner Res 2015; 30: 95-105.
24. Yin Y, Duan J, Guo C, Wei G, Wang Y, Guan Y, et al. Danshensu accelerates angiogenesis after myocardial infarction in rats and promotes the functions of endothelial progenitor cells through SDF-1α/CXCR4 axis. Eur J Pharmacol 2017; 814: 274-282.
25. Wang Y, Luther K. Genetically manipulated progenitor/stem cells restore function to the infarcted heart via the SDF-1α/CXCR4 signaling pathway. Prog Mol Biol Transl Sci 2012; 111: 265-284.
26. Yu P, Zhang Z, Li S, Wen X, Quan W, Tian Q, et al. Progesterone modulates endothelial progenitor cell (EPC) viability through the CXCL12/CXCR4/PI3K/Akt signalling pathway. Cell Prolif 2016; 49: 48-57.
27. Ito M, Shichinohe H, Houkin K, Kuroda S. Application of cell sheet technology to bone marrow stromal cell transplantation for rat brain infarct. J Tissue Eng Regen Med 2017; 11: 375-381.
28. Sasagawa T, Shimizu T, Yamato M, Okano T. Endothelial colony-forming cells for preparing prevascular three-dimensional cell-dense tissues using cell-sheet engineering. J Tissue Eng Regen Med 2016; 10: 739-747.

29. Shudo Y, Cohen JE, Macarthur JW, Atluri P, Hsiao PF, Yang EC, et al. Spatially oriented, temporally sequential smooth muscle cell-endothelial progenitor cell bi-level cell sheet neovascularizes ischemic myocardium. Circulation 2013; 128: S59-S68.
30. Michler RE. The current status of stem cell therapy in ischemic heart disease. J Card Surg 2018; 33: 520-531.
31. Yu H, Lu K, Zhu J, Wang J. Stem cell therapy for ischemic heart diseases. Br Med Bull 2017; 121: 135-154.
32. Wang S, Zhou C, Zheng H, Zhang Z, Mei Y, Martin JA. Chondrogenic progenitor cells promote vascular endothelial growth factor expression through stromal-derived factor-1. Osteoarthritis Cartilage 2017; 25: 742-749.
33. Chen G, Fang T, Qi Y, Yin X, Di T, Feng G,et al. Combined Use of Mesenchymal Stromal Cell Sheet Transplantation and Local Injection of SDF-1 for Bone Repair in a Rat Nonunion Model. Cell Transplant 2016; 25: 1801-1817.
34. Hwang S, Zimmerman NP, Agle KA, Turner JR, Kumar SN, Dwinell MB. E-cadherin is critical for collective sheet migration and is regulated by the chemokine CXCL12 protein during restitution. J Biol Chem 2012; 287: 22227-22240.
35. Kim SW, Jin HL, Kang SM, Kim S, Yoo KJ, Jang Y, et al. Therapeutic effects of late outgrowth endothelial progenitor cells or mesenchymal stem cells derived from human umbilical cord blood on infarct repair. Int J Cardiol 2016; 203: 498-507.
36. Xu S, Zhu J, Yu L, Fu G. Endothelial progenitor cells: current development of their paracrine factors in cardiovascular therapy. J Cardiovasc Pharmacol 2012; 59: 387-396.
37. Abe Y, Ozaki Y, Kasuya J, Yamamoto K, Ando J, Sudo R,et al. Endothelial progenitor cells promote directional three-dimensional endothelial network formation by secreting vascular endothelial growth factor. PLoS One 2013; 8: e82085.
38. Deng Y, Wang J, He G, Qu F, Zheng M. Mobilization of endothelial progenitor cell in patients with acute ischemic stroke. Neurol Sci 2018; 39: 437-443.

Tables

Table 1
Primer pairs used for reverse transcription -quantitative PCR

Gene	Forward (5’-3’)	Reverse(5’-3’)
CXCR4	CTTTCTTTGCCTGCTGGCTACCG	CTCCGTGATGGAGATCCACTTGTGC
PI3K	ATGGCTCATACAGTTCGGAAAGAC	AGCACTCAGTTACAGAGGGTGGG
AKT	GATCATGCAGCACCGCTTCTTTG	CAGGCTGTGCCACTGGCTGAGTA
eNOS	TTTGTCTGCGGTGATGTCACTATGGC	GGTGTTTCTTGGGTAGGCGGGTC
β-actin	AGGGAAATCGTGCGTGACAT	CCTCGGGGCATCGGAA

Figures

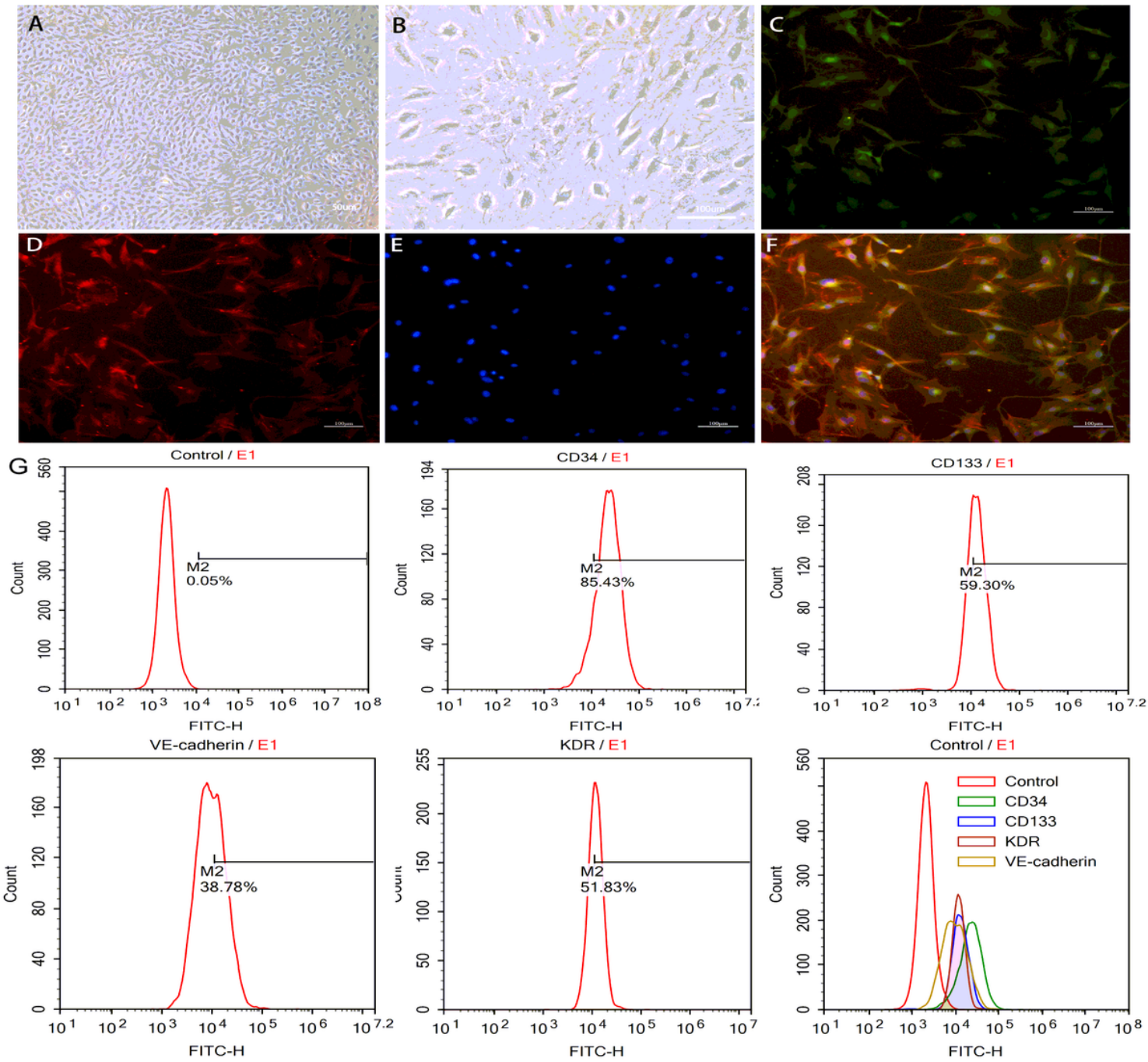

Figure 1

Isolation and characterization of rat bone marrow-derived endothelial progenitor cells (EPCs). (A): The BM-EPCs were arranged in a cobblestone-like pattern after 7 days of cultivation (magnification 100x). (B): Some EPCs were arranged in an island-like pattern (magnification 200x). (C): BM-EPC uptake of FITC-UEA-1 could be visualized (green). (D): EPC uptake of DiI-Ac-LDL could be visualized (red). (E): DAPI was used to stain the nucleus (blue). (F): The double-stained cells for DiI-Ac-LDL (red) and FITC-UEA-1 (green) exhibit yellow fluorescence. (G): Flow cytometry analysis of surface markers of BM-EPCs. Positive staining of CD34/CD133/VE-cadherin/KDR.

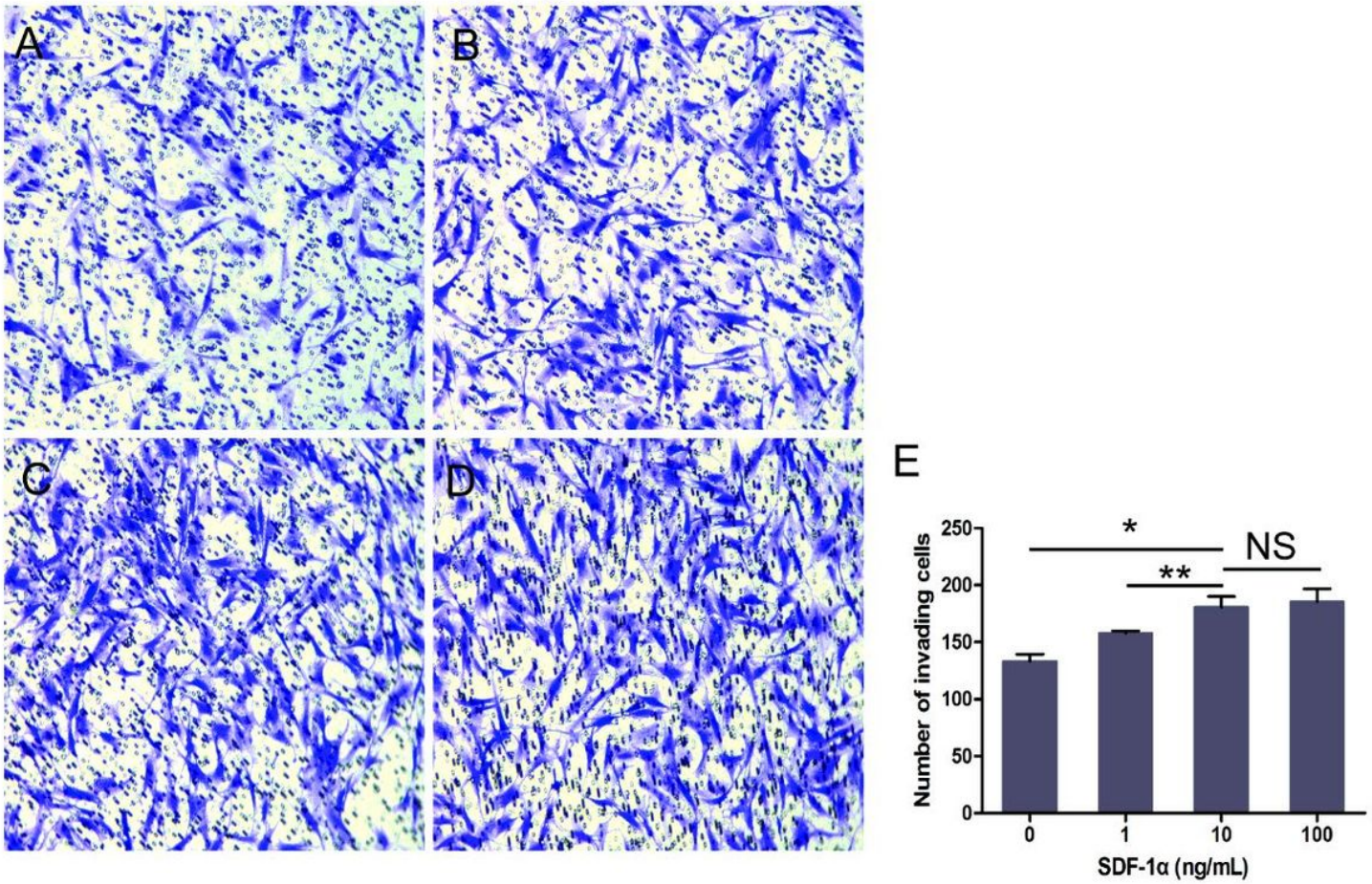

Figure 2

Transwell assay of BM-EPC migration toward different concentrations of SDF-1α (0, 1, 10 and 100 ng/mL). (A): Under non-SDF-1α conditions, BM-EPCs were able to migrate through the filter at a low rate. (B): BM-EPCs were able to migrate through the filter at a higher rate under non-SDF-1α conditions than under 1 ng/mL SDF-1α conditions. (C): Under 10 ng/mL SDF-1α conditions, BM-EPCs migrated through the filter at the fastest rate. (D). Compared with 10 ng/mL SDF-1α conditions, BM-EPCs migrated through the filter at a rate no different than that observed under 100 ng/mL SDF-1α conditions. (E) Number of BM-EPCs migrating through the filter (cells per field of view). (n=6 per group; *p<0.001, **p<0.01, NS, not significant)

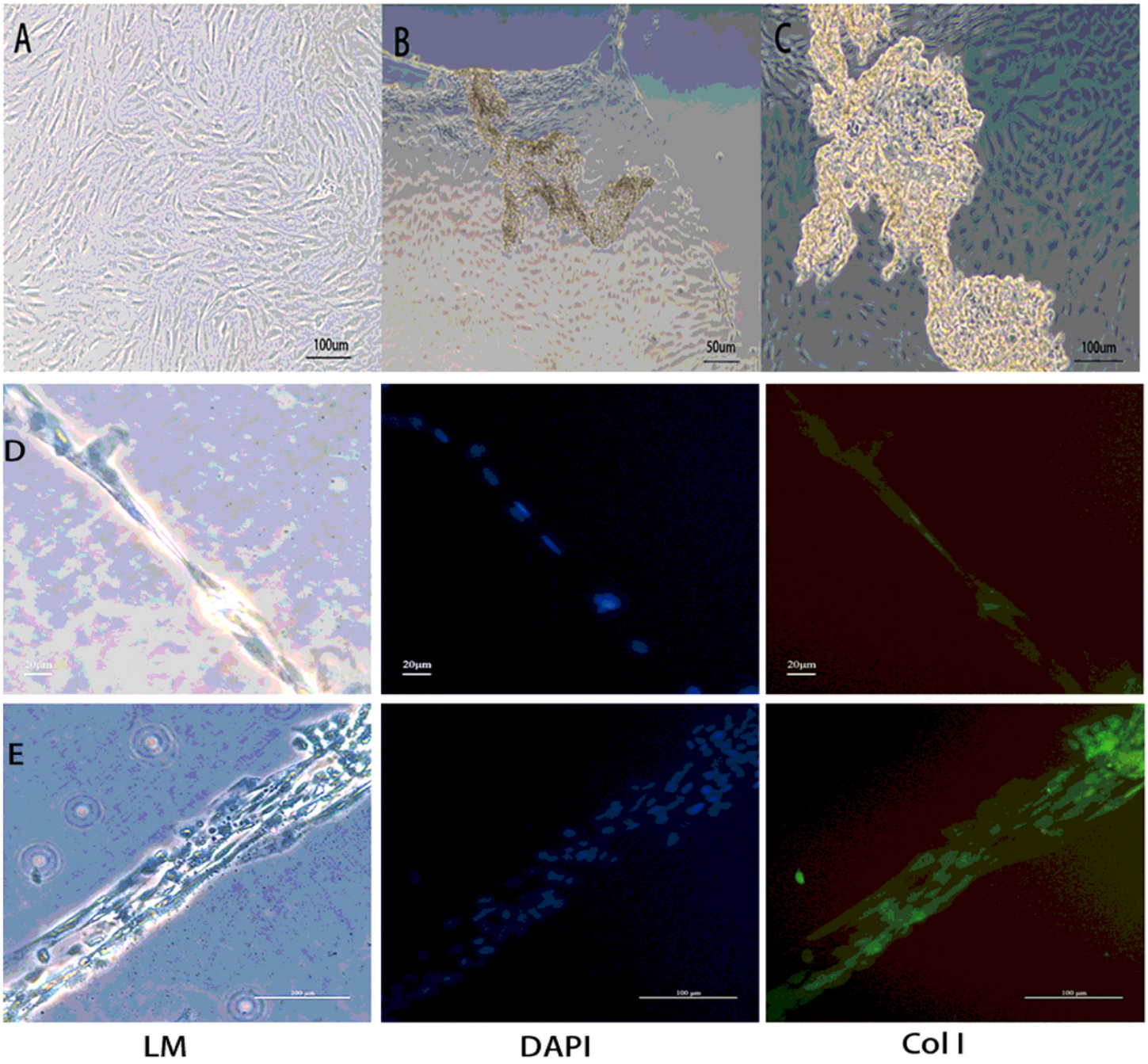

Figure 3

Gross examination of BM-EPC sheets. (A): The BM-EPC cells in the cell sheet are arranged more closely under the microscope. (B): Photograph of a monolayered BM-EPC cell sheet. (C): Photograph of a multilayered BM-EPC cell sheet. (D): The monolayered BM-EPC cell sheet, from left to right, under a light microscope (LM), with DAPI to stain the nucleus (blue), and with anti-Collagen I to stain the cytoplasm (green). (E): The multilayered BM-EPC cell sheet, from left to right, under a light microscope (LM), with DAPI to stain the nucleus (blue), and with anti-collagen I to stain the cytoplasm (green).

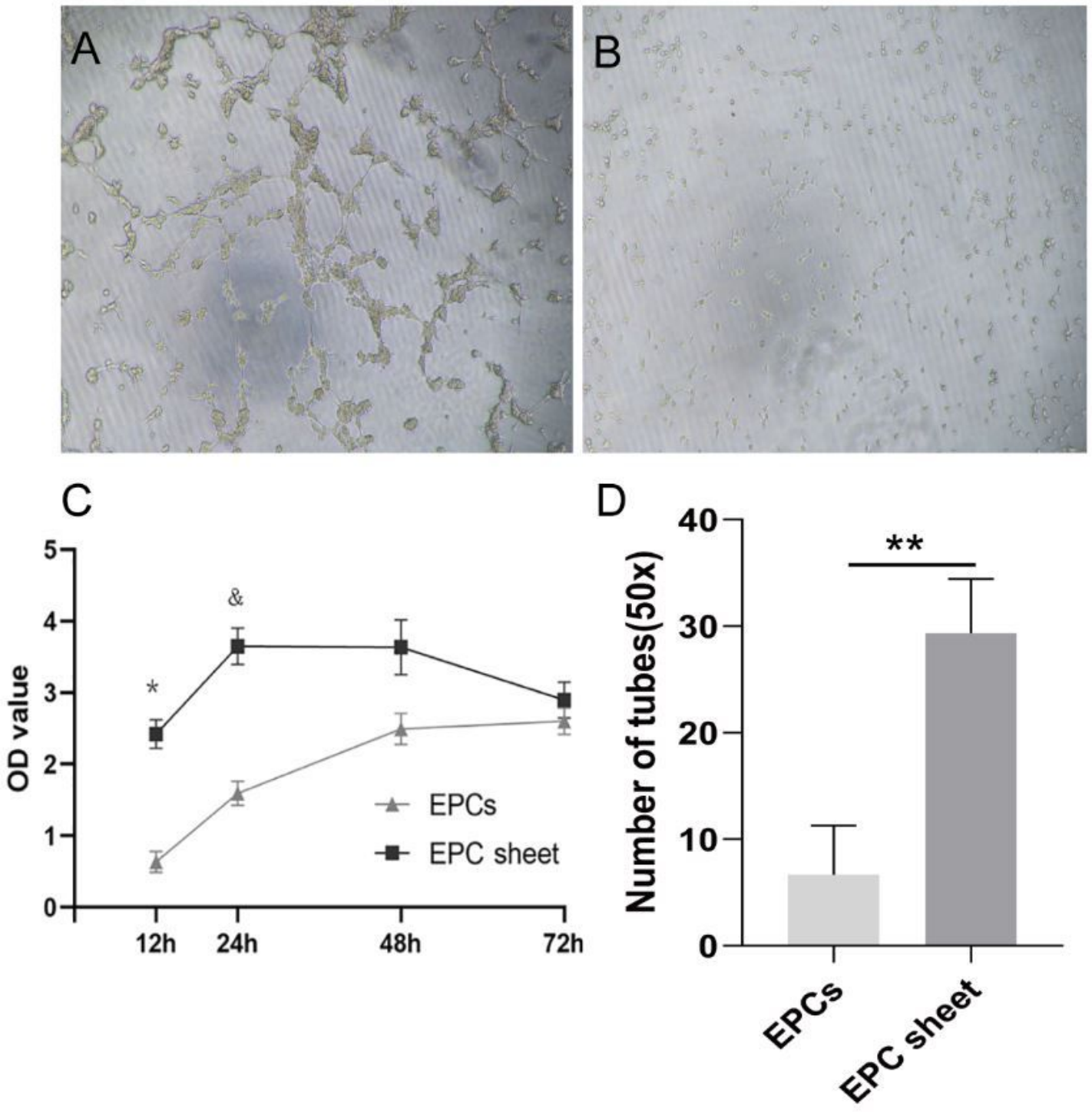

Figure 4

Comparison of BM-EPC cell sheets and single cells in suspension in proliferation and tube formation assays in vitro. (A): BM-EPC cell sheet tube formation. (B): Single-cell BM-EPC suspension tube formation (magnification 100×). (C): Quantitative analysis of the proliferation of BM-EPC cell sheets and BM-EPC single cells (&p<0.01 *p<0.001 vs single cells, n=18). (D): Quantitative analysis of tube formation by BM-EPC cell sheets and BM-EPC single cells (**p=0.004<0.05; n=6 per group).

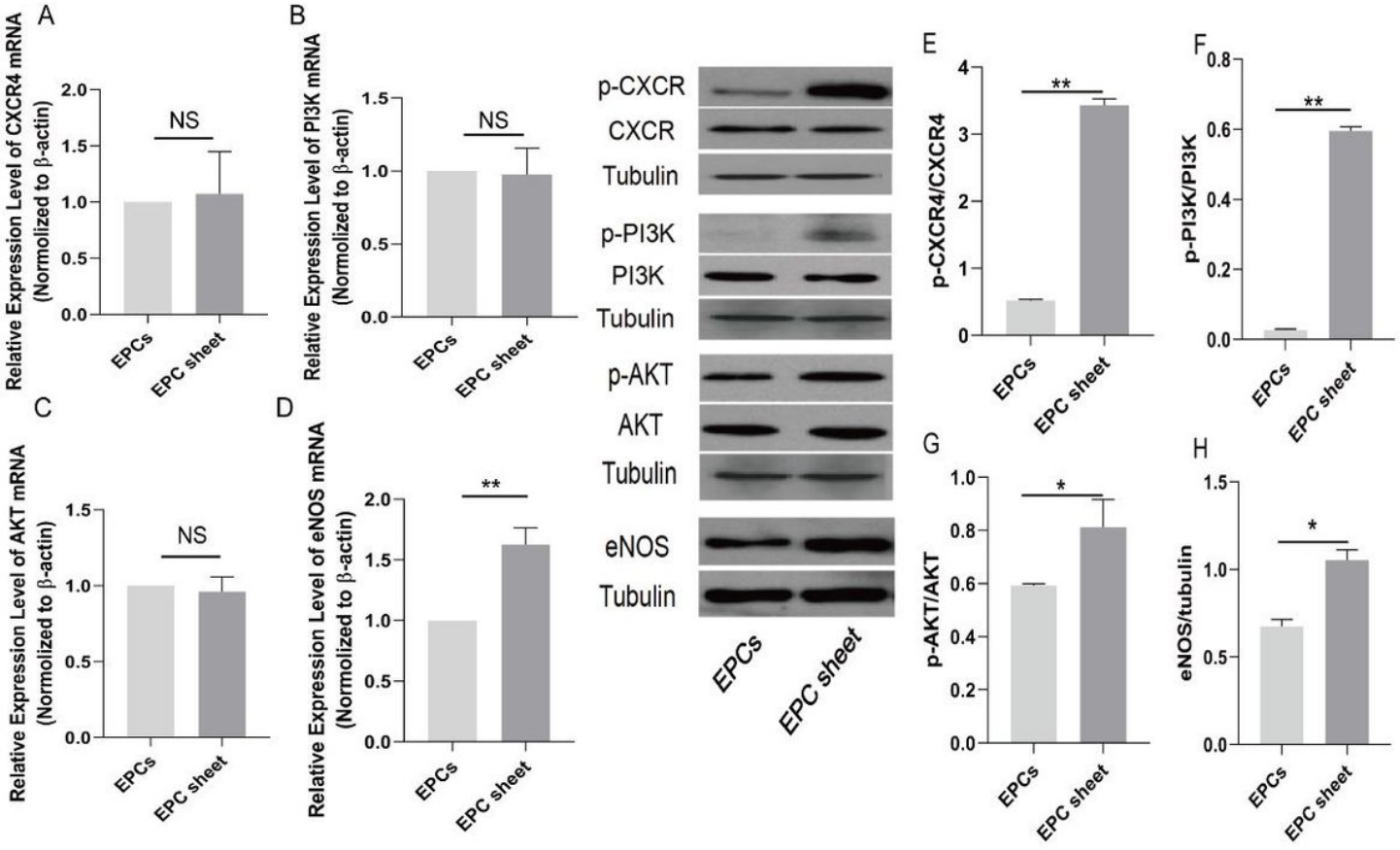

Figure 5

RT-PCR and western blotting analysis of the expression of CXCR4, as well as PI3K/AKT/eNOS signaling pathway components, in BM-EPC cell sheets and BM-EPC single-cell suspensions. (A-C): The mRNA levels of CXCR4, PI3K and AKT were basically unchanged. (D): Compared with that of the control group, the mRNA level of eNOS was significantly higher in the BM-EPC cell sheet. (E-G): The p-CXCR4/CXCR4, p-PI3K/PI3K and p-AKT/AKT ratios were higher in the BM-EPC cell sheet than in cells in suspension. (H): The protein expression of eNOS in the BM-EPC cell sheet was significantly higher than that in the BM-EPC single-cell group. (n=6, per group; **p=0.001<0.05, *p<0.05; NS, not significant)

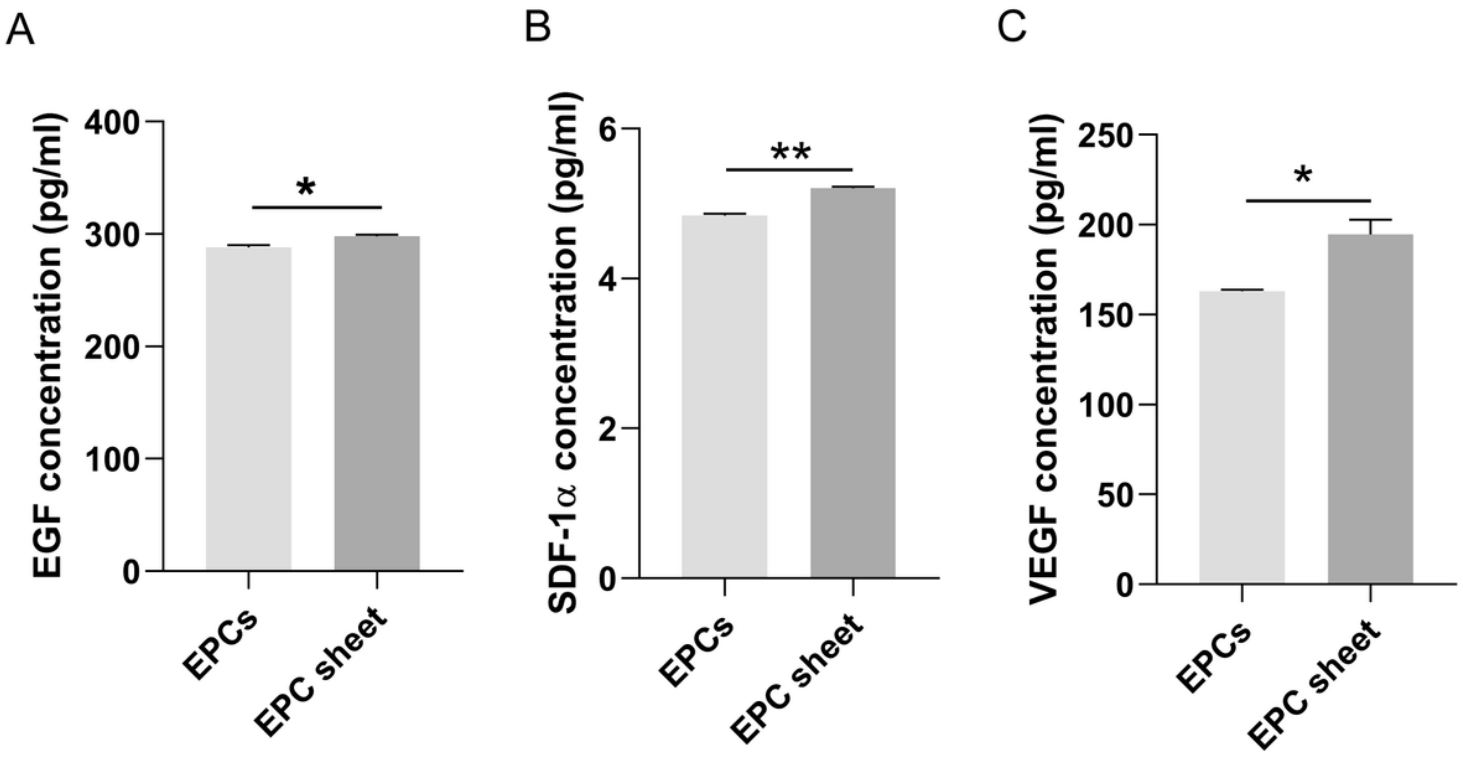

Figure 6

ELISA was used to determine the concentrations of the paracrine factors VEGF, EGF and SDF-1α in the cell culture medium. (A): The BM-EPC cell sheet secreted more of the paracrine factor EGF than did the BM-EPC single-cell group. (B): The BM-EPC cell sheet secreted more of the paracrine factor SDF-1α than did the BM-EPC single-cell group. (C): The BM-EPC cell sheet secreted more of the paracrine factor VEGF than did the BM-EPC single-cell group (n=6, per group; **p<0.001, *p<0.01)